

# Development of mullite and spinel coatings on graphite for improved water-wettability and oxidation resistance

Sk.A. Ansar<sup>a</sup>, S. Bhattacharya<sup>b</sup>, S. Dutta<sup>a</sup>, S.S. Ghosh<sup>a</sup>, S. Mukhopadhyay<sup>a,\*</sup>

<sup>a</sup>Department of Chemical Technology, Calcutta University, 92 APC Road, Kolkata 9, India

<sup>b</sup>Calcutta Institute of Engg. and Management, 24/1A C. G. Road, Kolkata 40, India

Received 15 June 2009; received in revised form 24 February 2010; accepted 17 March 2010

Available online 29 April 2010

## Abstract

Mullite and spinel forming sols were prepared from hybrid precursors having both organic and inorganic origins. Refractory grade graphite flakes were coated by these sols and their performances were compared in terms of oxidation resistance and water-wettability. Particle size distribution, structural evolution and related characteristics of both mullite and spinel gels have been investigated by dynamic light scattering (DLS), differential thermal analysis (DTA), X-ray diffraction (XRD) and infrared spectra (IR) studies. Coated graphites have also been studied by IR and XRD tests along with scanning electron microscopy (SEM) with energy dispersive spectral (EDS) analysis. The better performance of spinel coated graphite was confirmed. The mechanism of spinel formation on graphite was suggested to take place via intermediate gamma alumina phase formation from boehmite sol. It was clarified by DLS, XRD and microstructural analysis of dried and calcined gels.

© 2010 Elsevier Ltd and Techna Group S.r.l. All rights reserved.

**Keywords:** A. Sol–gel processes; D. Mullite; Spinel; Graphite

## 1. Introduction

Graphite is known to confer good resistance to wetting by molten metals and slags, high refractoriness, high thermal conductivity and work of fracture. As such it has been a potential candidate for composite refractories used in extreme environments [1]. However poor oxidation resistance and low water-wettability have always impeded its commercial application especially in monolithic refractories. Several methods have been tried therefore, to incorporate graphite in castable refractories although some technical limitations still exist to develop flawless monolithic refractory containing graphite. Among various routes, the formation of thin film over graphite has been the subject of research of a lot of eminent people working in this area [2–5]. Consequently, a lot of publications report the surface modification of graphite by the coatings of alumina ( $\text{Al}_2\text{O}_3$ ), titania ( $\text{TiO}_2$ ), silica ( $\text{SiO}_2$ ), etc. obtained from a variety of precursors. Apart from single oxide coatings the synthesis and characterization of binary oxide

coatings over graphite have also been attempted [6], but very often these investigations include expensive organometallics and no specific data is available on the coating thickness and the performance of composites prepared with it [2]. However, both these papers substantiated the antioxidation behaviour and improvement of wettability of the coated graphite by contact angle measurement, electro kinetic studies, thermogravimetry, etc. Yilmaz et al. prepared boehmitic alumina-coated graphite by sol–gel method but no specific explanation of coating formation mechanism was depicted. They showed that the heating speed of the coating process was an important parameter and the sol coating wetted the graphite borders more efficiently than the surface [7]. Some researchers used antioxidant powders (e.g. Al, Si) in graphite containing materials although they caused extensive hydration of the refractory and release of explosive gases [4]. From the refractory point of view, it is also known that antioxidant like Al in MgO–C refractory is not suitable to be used in the melting of Fe–Mn–Al alloy steels [8].

Mullite and spinel gels synthesized by several researchers are known to produce a new generation bonds within the matrix of refractory composites which are water compatible at low temperature, less expensive and capable to form bonds at low

\* Corresponding author.

E-mail address: [msunanda\\_cct@yahoo.co.in](mailto:msunanda_cct@yahoo.co.in) (S. Mukhopadhyay).

temperature [9]. These two binary oxide coatings are important ceramic materials which may be used to coat the graphite surface efficiently to improve the water affinity and oxidation resistance of the latter. The bonding mechanism if investigated properly, the coated graphite may be incorporated in refractory composites for both ferrous and non-ferrous metallurgical conditions. In our previous paper [10], the development of a very low cost spinel coating on graphite has been discussed. Although it improved the slag performance of a high alumina castable, but the particulate type sol–gel spinel showed some discontinuities of that coating over the graphite flakes. For this purpose, in this work a hybrid polymeric precursor of spinel has been used to retain the integrity of the coating without much raising the cost factor. The mullite precursor has also been prepared by a similar hybrid polymeric route to coat the graphite flakes. Some authors suggested [11] the failure of mullite bond towards full protection of graphite from oxidation, whereas some authors opine [12] that thin mullite overcoat on graphite reduces the chances of oxidation especially at 1000 °C. Apart from sol–gel, other methods for mullite coating (from alumina–silica composite film) on graphite have been reported [13] but the method involves a costly CVD technique.

This paper describes the synthesis and characterization of mullite and spinel coated graphite for possible usage in refractory composites. The phase evolutions of mullite and spinel gels prepared from suitable precursors have also been studied to correlate the performance of both the coatings on graphite. The microstructural assemblage, infrared studies, etc. were done to corroborate their performance. Water holding character of coated graphite was studied by a ‘Pressure Plate Extractor’ method [14] as done by soil scientists.

## 2. Experimental

Both the binary (mullite and spinel forming) sols were prepared by a hybrid polymeric route, keeping the commercial point in mind. For this purpose, one ingredient of the binary material was taken from the alkoxide origin whereas the other precursor was from cheaper origin like metal nitrate (LR grade). For spinel sol (code: G') preparation, aluminium-sec-butoxide and hydrous magnesium nitrate were used, whereas for mullite sol (code: M), tetraethylorthosilicate (TEOS) and hydrous aluminum nitrate were taken. The evolution of mullite and spinel crystalline phases has been identified by infrared (IR) and X-ray diffraction (XRD) studies at increasing temperatures. The differential thermal analysis (DTA) of both the gels was examined to substantiate the respective XRD patterns. The dynamic light scattering (DLS) of both the sols were done to understand the particle size of coating over the graphite surface. Dynamic light scattering of sols were carried out in Malvern instrument (DTS Ver. 5.00), MAL 1010871 and Model BI 200 SM-Goniometer (Ver. 2.0), MELLES GRIOT HeNe-LASER Terbo-Corr Correlator. Differential thermal analysis was done in Shimadzu DT-40 and Netzsch models in air at a rate of 10 °C/min.

Refractory grade natural flaky graphite powder (Fig. 1a) having 92% fixed carbon, 6% ash content, 2% volatile matter

and particle size below 200 µm has been selected for this investigation. The powder was subjected to XRD phase analysis using a ‘Philips Analytical Instrument’ with a Ni-filtered Cu K $\alpha$  radiation at 40 kV/20 mA. For microstructural studies, scanning electron microscopy (SEM with EDS) experiment was conducted with the instruments/models JEOL JSM 5200 and Hitachi S-3400N.

Using a REMI Magnetic Stirrer, 200 g of supplied graphite was very slowly mixed to the precursor sol, gradually increasing the speed to 2000 rpm. The quantity of both mullite and spinel coating was equivalent to 1.7 wt.% and the mixing operation was carried out in 1 h. The washed slurry of coated graphite was aged in air at room temperature for 24 h and dried in vacuum oven at 110 °C for another 24 h. The mass was then calcined to 600 °C at a moderately fast heating rate and soaked for 24 h. After normal cooling, coated graphite was sieved to requisite fineness (Fig. 1b, done in Malvern Mastersizer E.Ver. 1.2b model) for application in a refractory composite. Spinel coated graphite and mullite coated graphite were named respectively as G'C and MC. The characteristics of these coated graphites along with the uncoated one were compared by XRD, IR, oxidation resistance and water-wettability (i.e., moisture-retention) test. Examination of the calcined coatings formed on graphite surface was conducted also by SEM supplemented with energy dispersive analysis (EDS).

Oxidation resistance test of the as-received graphite was performed at 600, 900 and 1200 °C by taking 5 g sample in each case, heating them at 10 °C/min and holding for 1 h. After natural cooling the weight loss at each temperature was measured to calculate the oxidation ratio (%) [2]. The water-wettability of graphite was examined by the ‘Pressure Plate Extractor (5 bar)’ apparatus of ‘Soil Moisture Equipment Corporation’, USA. The principle of this test was similar to that applied for determining the water holding characteristics of soil–water system [14].

The root cause of the betterment of spinel coating, i.e., evolution of superfine boehmite (i.e., precursor of nanostructured  $\gamma$ -Al<sub>2</sub>O<sub>3</sub>) at 300 °C from the respective sol has been confirmed by XRD studies. In this regard the particle size distributions of boehmite sol and SEM (with EDS) of both the dried (200 °C) and calcined (1400 °C) gels have also been performed.

## 3. Results and discussion

The XRD pattern of the as-received graphite showed the characteristic peak at around 27° and 55° [10]. The SEM micrograph in Fig. 1a shows its grains varying mostly in between 20 and 100 µm and they are agglomerated.

Fig. 2(a and b) shows the particle size distribution of mullite and spinel forming sols, respectively. It is clear that the hybrid aquo-polymeric composite units are finer in the spinel sol. Although some nanodimensional particles exist in the mullite sol, the average size distribution of the spinel is on the finer side. It may be anticipated then that the evolution of the spinel with thermal treatment would be easier from the spinel precursor. Fig. 2(c and d) shows the DTA analyses of

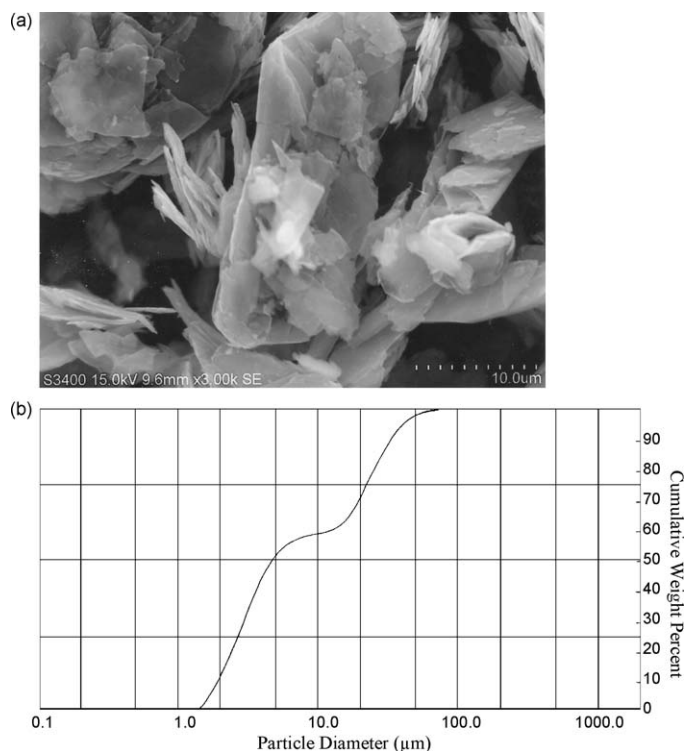


Fig. 1. (a) SEM micrograph of as-received graphite and (b) particle size distribution of coated graphites for refractory application.

respectively mullite and spinel gel fines. Fig. 2c shows the large endotherm above 150 °C due to release of chemically bonded water whereas the expulsion of physically held water starts at much lower temperature. The small endotherm nearby 260–280 °C may be due to melting of ammonium nitrate. The literature suggests [15] that the exotherm nearby 365–390 °C can be due to the bond formation between  $\text{Al}_2\text{O}_3$  and  $\text{SiO}_2$ . The sharp exotherm at 964 °C may indicate the transformation of predominantly monophasic gel to either tetragonal or cubic mullite. In that case the small exotherm at 1235 °C is due to orthorhombic mullite formation. Fig. 2d shows a broad endotherm at ~90 °C due possibly to the loss of adsorbed water and removal of other volatiles. The small exotherm at ~285 °C can be due to the decomposition of nitrates. The broad exotherm nearby 350 °C would definitely be due to the oxidation of organic compounds (e.g. butanoic acid) together with the decomposition of hydroxides. The TG curve (not displayed) showed that ~60% weight loss takes place up to 600 °C, after which the weight loss is very low. From the literature, it is known that the spinel phase is well crystallized above 600 °C [16,17]. In some cases it has been found to be a mixture of cubic and monoclinic spinel before 800 °C [18] after which it is totally converted to cubic phase. The very small peak nearly 870 °C may therefore indicate the complete conversion of (spinel) cubic phase. So it may be suggested that  $\gamma\text{-Al}_2\text{O}_3$  and MgO phases start forming spinel at above 500 °C, however the evolution of spinel is complete at ~870 °C. Fig. 3(a and b) shows the evolution of crystalline phases in mullite and spinel

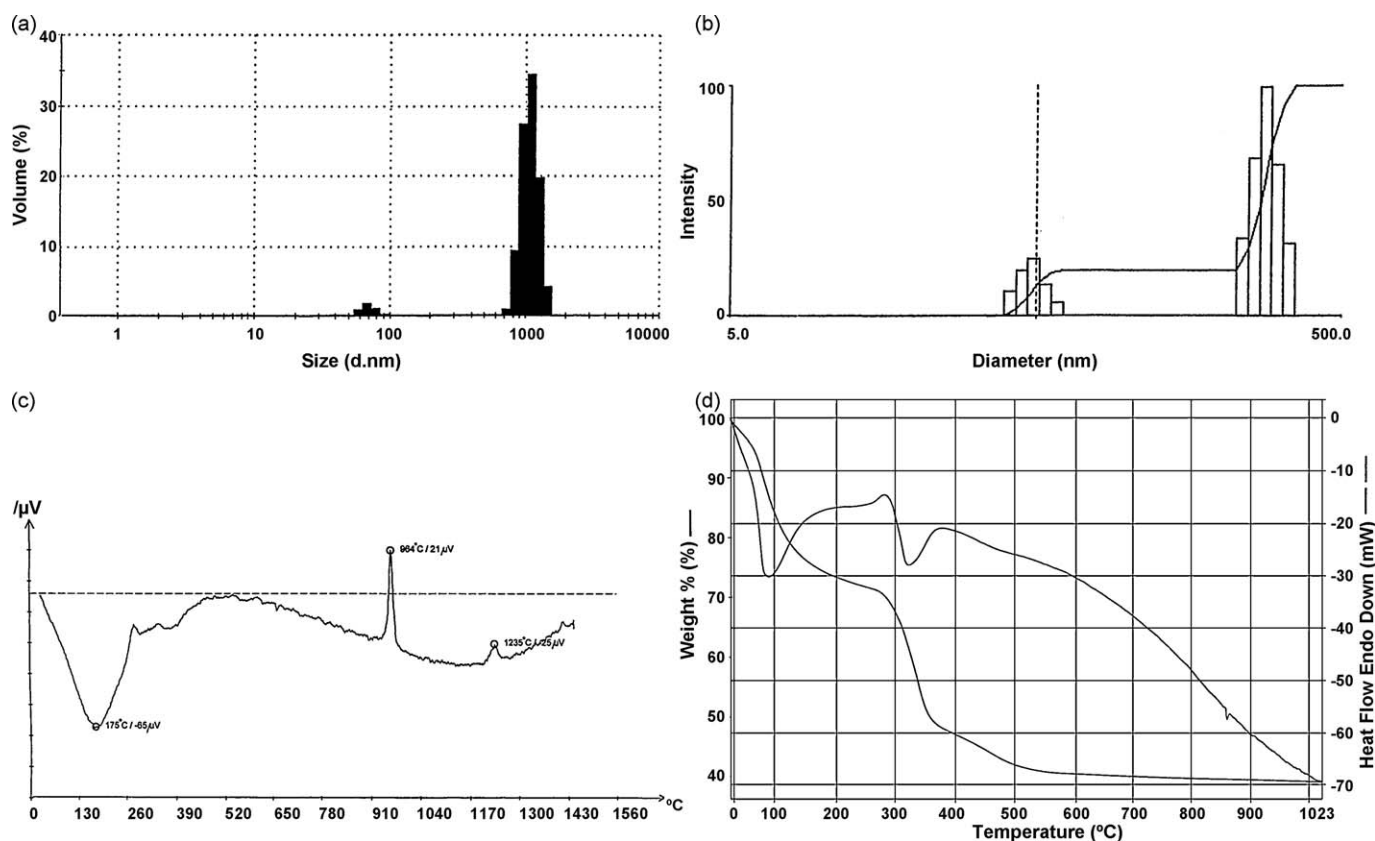


Fig. 2. (a and b) Particle size distribution of respectively mullite and spinel forming sols. (c and d) DTA analyses of respectively mullite and spinel gels.

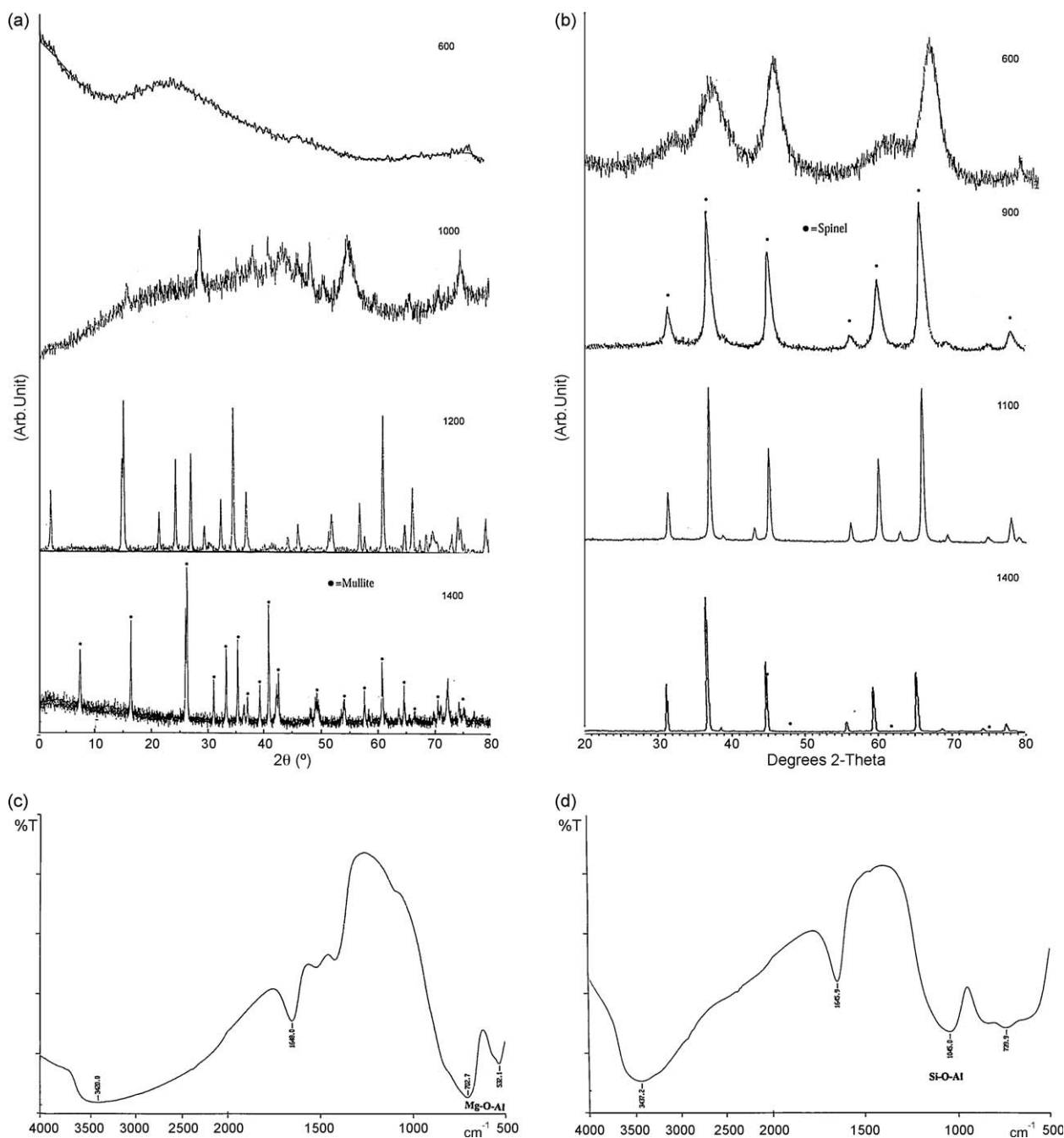


Fig. 3. (a and b) Evolution of the crystalline phases respectively in mullite (600, 1000, 1200, 1400 °C) and spinel gels (600, 900, 1100, 1400 °C) with increasing temperature. (c and d) IR patterns of respectively spinel and mullite gels calcined at 900 °C.

finer with increasing calcination temperature, respectively. In Fig. 3a, the XRD traces of mullite infer that it is poorly crystalline even at 1000 °C, whereas at 1200 °C and above, the orthorhombic mullite phases become prominent. It is interesting that although the mullite synthesis route resembles co-precipitation [15], yet the finer scale mixing of the constituents turns some part of gel to be a monophasic one. It may be noted from Fig. 3b that the spinel phase is well crystallized at 900 °C. From the intensities of (3 1 1), (4 0 0) and (4 4 0) planes [19], it may be suggested that from 600 °C onwards microcrystalline Mg-doped  $\gamma$ - $\text{Al}_2\text{O}_3$  phases topochemically convert to spinel crystallites. In Fig. 3c, the IR pattern of spinel fine calcined at

900 °C clearly reveal the strong Mg–O–Al linkage at 700 and 530  $\text{cm}^{-1}$ , confirming the spinel ( $\text{MgAl}_2\text{O}_4$ ) evolution. In Fig. 3d, the IR pattern of mullite gel calcined at 900 °C shows the formation of Si–O–Al linkage pertaining to the band at 1045  $\text{cm}^{-1}$ . However the bands at 3437, 1645 and 739  $\text{cm}^{-1}$  suggest that a lot of silanol groups, Al–O linkage, water and ethanol are still present in the calcined gel. All these conclude the amorphous and diphasic nature of the aluminosilicate powder. In that case the corresponding DTA peaks at above 900 °C (Fig. 2c) may be assigned to  $\gamma$ - $\text{Al}_2\text{O}_3$  formation and that at 1235 °C due to mullite formation. Therefore, for spinel coating, the evolution of Mg-doped  $\gamma$ - $\text{Al}_2\text{O}_3$  over graphite may

be expected after heat treatment at 600 °C; but for mullite coating the Si–O–Al linkage has been formed well although the coating remains amorphous.

Fig. 4(a and b) shows the IR patterns of as-received, spinel coated (G'C) and mullite coated graphite (MC). In Fig. 4b bands at 3438 and 1650  $\text{cm}^{-1}$  confirm the association of more (OH) groups in coated graphites compared to as-received graphite (Fig. 4a). These two peaks, if carefully noted, reveal that spinel coating is associated with more hydrophilic (OH) groups than mullite. At the same time the sharp hydrophobic band at  $\sim 770 \text{ cm}^{-1}$  (i.e., =C–H linkage) in uncoated graphite has been significantly masked by the spinel coating. The Si–O–Al linkage ( $1067 \text{ cm}^{-1}$ ) is clear in mullite coated graphite along with the presence of hydrophobic linkage of graphite at  $771 \text{ cm}^{-1}$ . As the spinel starts crystallizing from doped  $\gamma$ -

$\text{Al}_2\text{O}_3$  (Fig. 4c, band at  $720 \text{ cm}^{-1}$ ), it is evident that it prominently reduces the hydrophobic character of graphite. As  $\gamma\text{-Al}_2\text{O}_3$  behaves inherently as a strong Lewis acid [20], it can readily adsorb polar molecules to improve the water affinity of the coating. The betterment of spinel coating is also due to the presence of defects, which at 600 °C, may intercalate with the graphite structure [10].

Table 1 shows the oxidation ratio of two types of coated graphite after oxidation at 600, 900 and 1200 °C. It is clear that both the coatings improve the oxidation resistance of graphite to a large extent. Between these two, with increasing temperature, obviously the performance of spinel coating is better as the contact between graphite and atmospheric oxygen is inhibited effectively by the corresponding stable crystalline structure. At 600 °C, mullite performs slight better might be

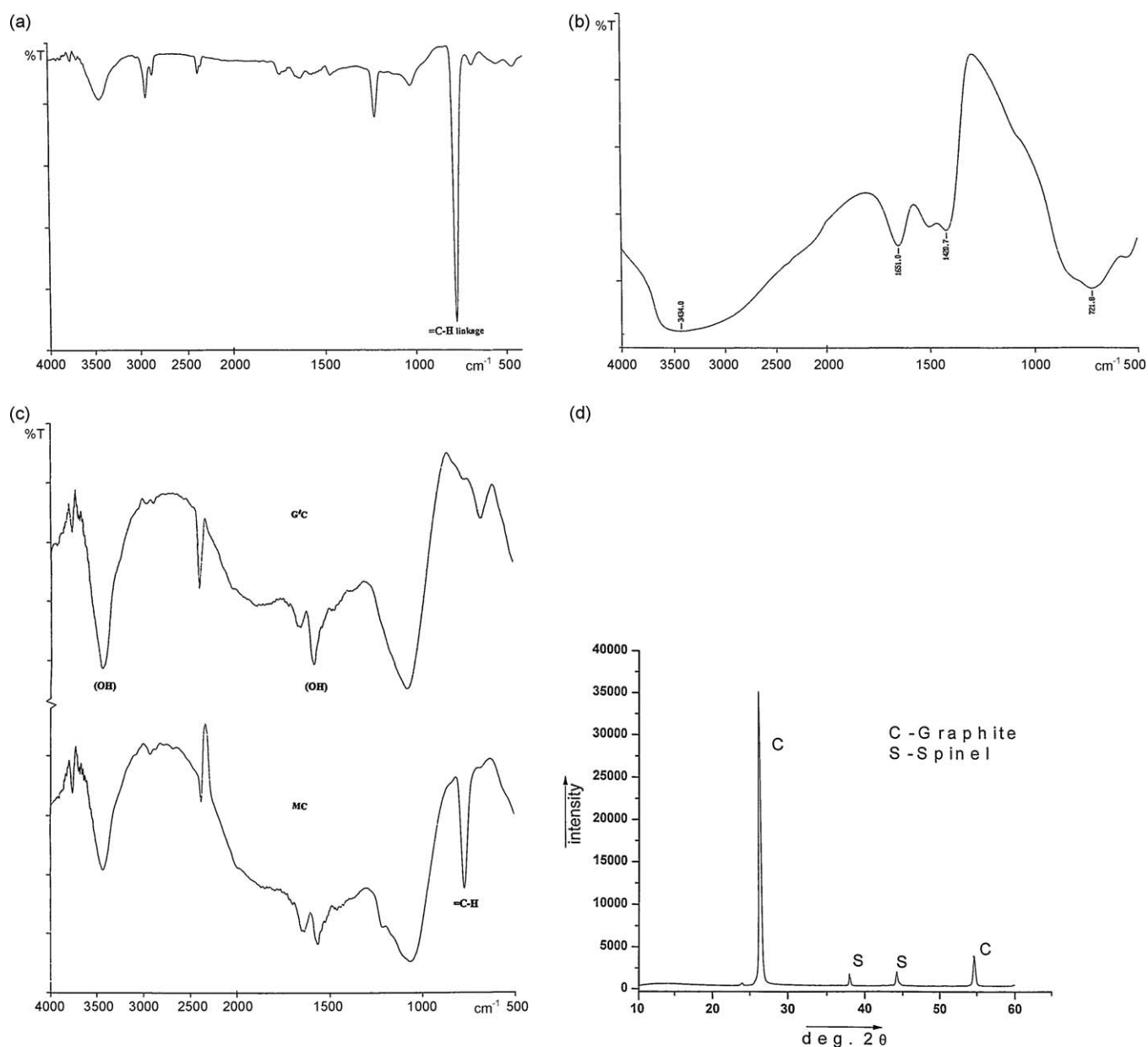


Fig. 4. IR patterns of (a) as-received graphite, (b) spinel gel calcined at 600 °C (code: G'6), (c) spinel coated (G'C) and mullite coated graphite (MC) and (d) XRD pattern of spinel coated graphite (G'C).



Table 1  
Oxidation resistances of coated and uncoated graphites.

Temperature (°C)	Oxidation ratio of graphite (%)		
	Uncoated	Spinel coated (G'C)	Mullite coated (MC)
600	12.0	5.0	7.2
900	30.0	7.5	10.6
1200	38.0	22	29.7

due to onset of crystallization of fine gamma alumina in the diphasic gel.

Fig. 4d shows the XRD of G'C, spinel coated graphite, which indicates that very fine spinel crystallites have been generated over the graphite flakes. They should be better represented as Mg-doped  $\gamma$ -Al<sub>2</sub>O<sub>3</sub> (generated from Mg-doped boehmite) which in due course of heating completely crystallizes topochemically to MgAl<sub>2</sub>O<sub>4</sub> phase [21]. The XRD report of MC (not displayed in this report), however, does not show any crystalline mullite phase for obvious reason.

Fig. 5(a and b) shows the SEM (with EDS) pattern of respectively mullite and spinel coated graphite. Both the compositions qualitatively show the presence of respectively (Si, Al) and (Mg, Al) elements with oxygen over the graphite

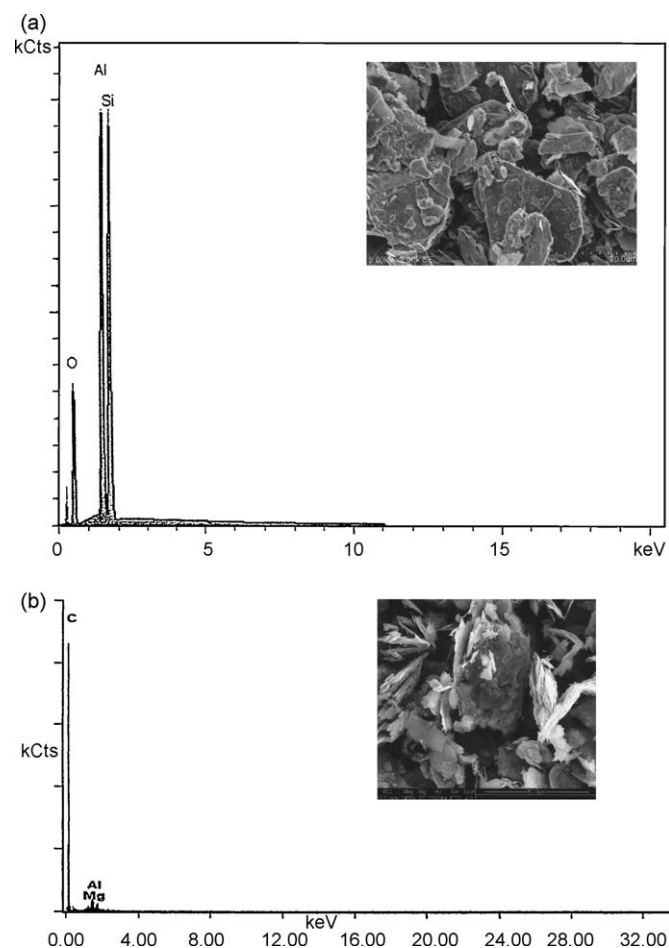


Fig. 5. (a and b) SEM (with EDS) micrographs of respectively mullite and spinel coated graphite flakes.

surface. The stoichiometry of spinel was closer to the theoretical than the mullite, might be due to the earlier crystallization in spinel forming sol. The tendency of mullite deposition at the border of the flakes was more prominent. The spinel coating being very thin and more uniform than mullite, the carbon underneath is also visible some in the respective EDS plot.

The pressure plate apparatus test shows that at atmospheric pressure,  $\sim 8.0\%$  (w/w) and  $5.0\%$  (w/w) improvement occurs respectively in the spinel and mullite coated materials, respectively. It can be well advocated then that the hydrophilicity and water holding properties considerably increase after coating formation over graphite.

From this comparative study it is apparent that spinel coating on graphite performs quite well and better than mullite. This can be attributed to the precursor boehmite sol (derived from Al sec-butoxide) utilized during spinel preparation. The boehmite sol results in gamma alumina after heat treatment [22–24], which inherently is a strong Lewis acid to absorb polar (water) molecules readily. The particle size of the sol (Fig. 6a) lies mostly in the nanometric range; it can easily generate nanostructured lamellar phases of boehmite to yield superfine  $\gamma$ -Al<sub>2</sub>O<sub>3</sub> crystallites after calcinations (Fig. 6b). The spinel phase prepared from this sol can easily grow up over the template of nanocrystalline  $\gamma$ -Al<sub>2</sub>O<sub>3</sub> phases (already generated) by fast diffusion of Mg<sup>2+</sup> ions in it. A large amount of interfacial area would thus be generated over graphite through which the defects of spinel could intercalate with the graphite substrate underneath [25]. In the microstructure of the boehmite derived spinel gel dried and calcined at respectively 200 and 1400 °C (Fig. 6c and d), it is observed that in the former, the microrelicts (EDS done at three regions) qualitatively retains the 2:1 stoichiometry of Al:Mg. The cracks and voids between the relicts of dried gel might have appeared due to the capillary stress during shrinkage and removal of volatiles. The microrelicts formed throughout the gel (Fig. 6c) still contain some amount of fugitives. Such precision in composition has been achieved due to the atomic scale mixing of the ingredients. On subsequent calcination those microrelicts yield defective nanocrystalline spinel with crystallite size below 30 nm. In our last publication [26], it has been documented that  $\gamma$ -Al<sub>2</sub>O<sub>3</sub> with incipient defective normal spinel character, is an important intermediate in this topochemical spinel forming reaction. Fig. 6d shows the microstructure of the same spinel calcined at 1400 °C. It has been corroborated (from the EDS plot taken at several regions) that the heated spinel retains the same (1:1) ratio between MgO and Al<sub>2</sub>O<sub>3</sub>. Hence the integrity of the coating could be retained by this cost effective spinel sol. At the same time, as the spinel phase crystallizes earlier than the mullite phase, the crystalline defects present in spinel coating would interact efficiently and earlier with the graphite structure to bond strongly over the substrate. The XPS study of the G'C gel also qualitatively confirm the 2:1 stoichiometry of Al:Mg over the graphite surface [10]. In this context the higher volume expansion of spinel must be considered to be an advantage to render compaction and compatibility with graphite coating; the unique feature of *in situ* spinel formation via sol gel route

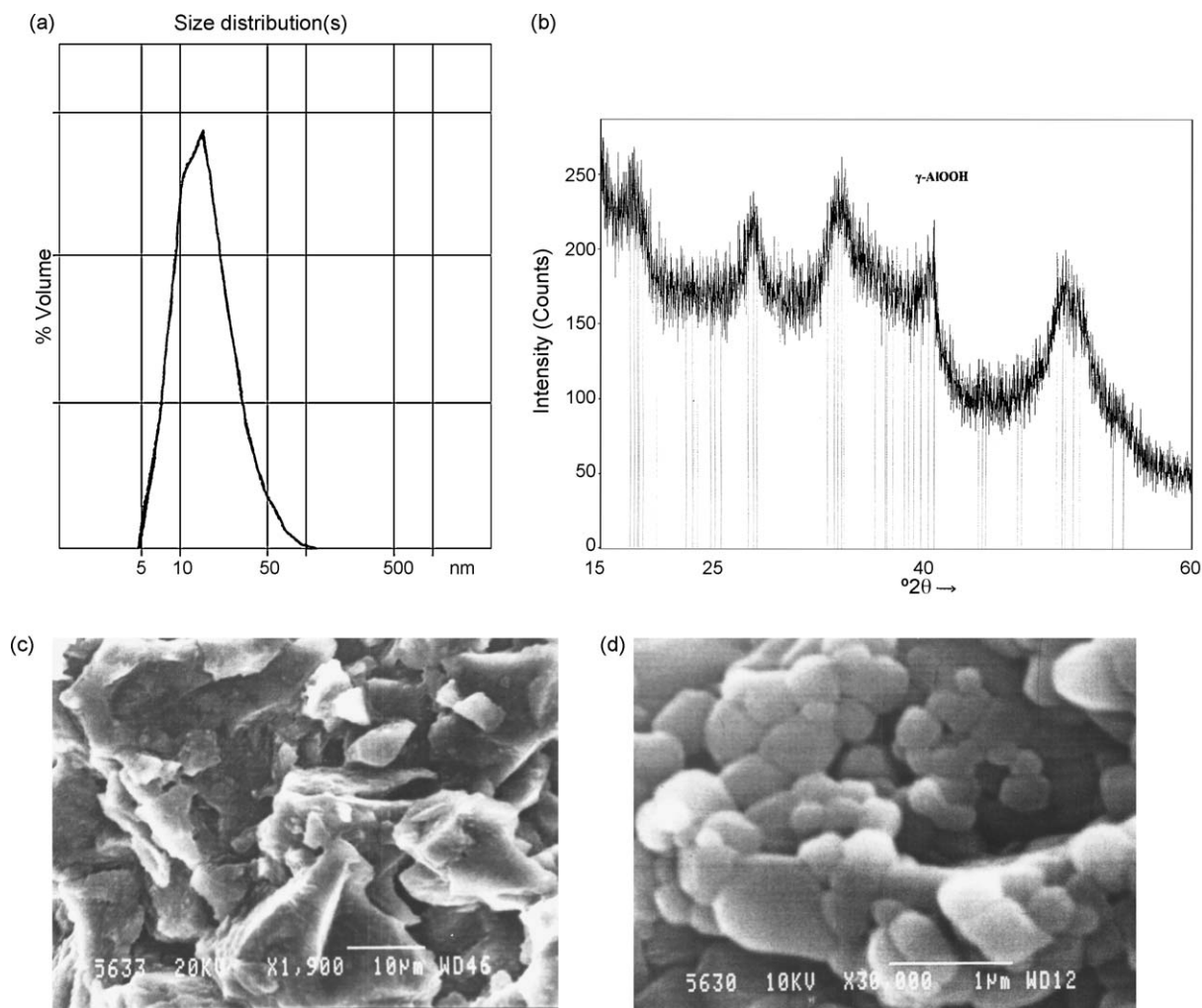


Fig. 6. (a) Particle size distribution of the boehmite sol utilized for spinel synthesis, (b) XRD pattern of nanosized  $\gamma$ - $\text{Al}_2\text{O}_3$  precursor on heating boehmite at 300 °C and (c) and (d) micrographs of the boehmite derived spinel gel heat treated respectively at 200 and 1400 °C.

therefore, can be helpful as it expands to reduce the void space in between the refractory and graphite [27].

#### 4. Conclusions

It may be concluded that:

- (1) Evolution of crystalline spinel occurs at much lower temperature (600 °C) than mullite (above 1200 °C) from the respective hybrid sols.
- (2) The oxidation resistance of spinel coated graphite at 600, 900 and 1200 °C was improved respectively to 5.0%, 7.5% and 22.0% and that of mullite coated graphite to 7.3%, 10.6% and 29.7%, both of which are better than as-received graphite 12.0%, 30.0% and 38.0%. The moisture-retention test inferred that water-wettability in spinel and mullite coated graphite have been increased respectively 8.0% and 5.0%.
- (3) The improvement of spinel coating and its evolution on graphite lies mainly on the nanostructured gamma alumina formation from the precursor boehmite gel with high surface area.

#### Acknowledgements

The authors thankfully acknowledge Prof. P.K. DasPoddar, Prof. T.K. Parya and Dr. P.K. Maiti, Department of Chemical Technology, Calcutta University for their help during the course of this work. The authors also express their sincere thanks to Prof. A.Patra, Dept. of Chemistry, Calcutta University.

#### References

- [1] S. Zhang, Next Generation Carbon-Containing Refractory Composites, Adv. in Sci. and Tech., vol. 45, Trans. Tech. Publications, Switzerland, 2006, pp. 2246–2253.
- [2] S. Zhang, W.E. Lee, Improving the water-wettability and oxidation resistance of graphite using  $\text{Al}_2\text{O}_3/\text{SiO}_2$  sol–gel coatings, J. Eur. Ceram. Soc. 23 (2003) 1215–1221.
- [3] S. Zhang, S. Hashimoto, W.E. Lee, Hydration of aluminium powder in magnesium-containing water, J. Am. Ceram. Soc. 85 (2005) 1057–1069.
- [4] A.R. Studart, M.D.M. Innocentini, I.R. Oliveira, V.C. Pandolfelli, Reaction of aluminium powder with water in cement-containing refractory castables, J. Eur. Ceram. Soc. 25 (2005) 3135–3143.
- [5] J. Yu, S. Ueno, K. Hiragushi, Improvement in flowability, oxidation resistance and water wettability of graphite powders by  $\text{TiO}_2$  coating, J. Ceram. Soc. Jpn. 104 (1996) 481–485.

- [6] (a) A. Saberi, F. Golestani-Fard, H. Sarpoolaky, M. Willert-Porada, T. Gerdes, R. Simon, C. Liebscher, Development of  $\text{MgAl}_2\text{O}_4$  spinel coating on graphite surface to improve its water-wettability and oxidation resistance, *Ceram. Int.* 35 (1) (2009) 457–461;  
(b) A. Saberi, F. Golestani-Fard, M. Willert-Porada, R. Simon, T. Gerdes, H. Sarpoolaky, Improving the quality of nanocrystalline  $\text{MgAl}_2\text{O}_4$  spinel coating on graphite by a prior oxidation treatment on the graphite surface, *J. Eur. Ceram. Soc.* 28 (2008) 2011–2017.
- [7] S. Yilmaz, et al., Synthesis and characterization of boehmitic alumina coated graphite by sol–gel method, *Ceram. Int.* 35 (5) (2009) 2029–2034.
- [8] J.W. Lee, J.G. Duh, High-temperature  $\text{MgO}$ – $\text{C}$ – $\text{Al}$  refractories–metal reactions in high-aluminum-content alloy steels, *J. Mat. Res.* 18 (2003) 1950–1959.
- [9] (a) S. Mukhopadhyay, S. Ghosh, M.K. Mahapatra, R. Majumdar, P. Barick, S. Gupta, S. Chakraborty, Easy-to-use mullite and spinel sols as bonding agents in a high alumina based ultra low cement castable, *Ceram. Int.* 28 (2002) 719–729;  
(b) S. Ghosh, R. Majumdar, B.K. Sinhamahapatra, R.N. Nandy, M. Mukherjee, S. Mukhopadhyay, Microstructures of refractory castables prepared with sol–gel additives, *Ceram. Int.* 29 (2003) 671–677.
- [10] S. Mukhopadhyay, et al., Spinel coated graphite for carbon containing refractory castables, *J. Am. Ceram. Soc.* 92 (8) (2009) 1895–1900.
- [11] G.D. Semchenko, I.Y. Shuteeva, O.N. Slepchenko, L.A. Angolenko, Protection of graphite and graphite-containing materials from oxidation, *Refract. Ind. Ceram.* 46 (4) (2005) 260–267.
- [12] O. Yamamoto, T. Sasamoto, M. Inagaki, Effect of mullite coating film on oxidation resistance of carbon materials with  $\text{SiC}$ -gradient, *J. Mat. Sci. Lett.* 19 (12) (2000) 1053–1055.
- [13] Z. Chen, M. Li, Y. Shi, Alumina–silica composite coatings on graphite by CVD at 550 °C, *J. Coat. Technol. Res.* 3 (3) (2006) 231.
- [14] E.C. Leong, S. Tripathy, H. Rahardjo, A modified pressure plate apparatus, *ASTM Geotech. Test. J.* 27 (2004) 322–331.
- [15] (a) A.K. Chakraborty, D.K. Ghosh, Synthesis and 980 °C phase development of some mullite gels, *J. Am. Ceram. Soc.* 71 (11) (1986) 978–987;  
(b) A.K. Chakraborty, Structural parameters of mullite formed during heating of diphasic mullite gels, *J. Am. Ceram. Soc.* 88 (9) (2005) 2424–2428.
- [16] J. Guo, H. Lou, H. Zhao, X. Wang, X. Zheng, Novel synthesis of high surface area  $\text{MgAl}_2\text{O}_4$  spinel as catalyst support, *Mat. Lett.* 58 (12–13) (2004) 1920–1923.
- [17] Z.Z. Chen, E.W. Shi, H.W. Zhang, Y. Zhang, X.B. Li, X.C. Liu, B. Xiao, Hydrothermal synthesis of magnesium aluminate platelets, *J. Am. Ceram. Soc.* 89 (12) (2006) 3635–3637.
- [18] M.K. Naskar, M. Chatterjee, Magnesium aluminate ( $\text{MgAl}_2\text{O}_4$ ) spinel powders from water-based sols, *J. Am. Ceram. Soc.* 88 (1) (2005) 38–44.
- [19] J.F. Pasquier, S. Komarneni, R. Roy, Synthesis of  $\text{MgAl}_2\text{O}_4$  spinel: seeding effects of formation temperature, *J. Mater. Sci.* 26 (1991) 3797–3802.
- [20] Y. Arai, *Chemistry of Powder Production*, Chapman and Hall, New York, 1996, pp. 49–70.
- [21] A. Kareiva, C. Jeff Harlan, D.B. MacQueen, R.L. Cook, A.R. Barron, Carboxylate-substituted alumoxanes as processable precursors to transition metal–aluminum and lanthanide–aluminum mixed-metal oxides: atomic scale mixing via a new transmetalation reaction, *Chem. Mater.* 8 (9) (1996) 2331–2340.
- [22] R.B. Bagwell, Gary L. Messing, Critical factors in the production of sol–gel derived porous alumina, *Key Eng. Mater.* 115 (1996) 45–64.
- [23] V. Saraswati, G.V.N. Rao, G.V. Rama Rao, Structural evolution in alumina gel, *J. Mater. Sci.* 22 (1987) 2529–2534.
- [24] L. Radonjic, L. Nikolic, Microstructural and sintering behaviour of magnesia doped, seeded, different boehmite derived alumina, *Ceram. Int.* 25 (1999) 567–575.
- [25] A.D. Mazzoni, M.A. Sainz, E.F. Aglietti, A. Caballero, Carbon coating and reaction on magnesia–alumina spinel, *Mater. Chem. Phys.* 101 (1) (2007) 211–216.
- [26] A. Banerjee, S. Das, S. Misra, S. Mukhopadhyay, Structural analysis on spinel ( $\text{MgAl}_2\text{O}_4$ ) for application in spinel bonded castables, *Ceram. Int.* 1 (2009) 371–380.
- [27] R.C. Bradt,  $\text{Mg}$ – $\text{Al}$  spinel: is it the mullite of 21st century? *Refract. Appl. News* 9 (4) (2004) 8–9.